Organometallics 1987, *6*, 1219–1226

Intramolecular C–H Bond Activation of Benzyl Ligands by Metalated Cyclopentadienyl Derivatives of Permethylhafnocene. Molecular Structure of $(\eta^5\text{-}C_5Me_5)(\eta^5,\eta^1\text{-}C_5Me_4CH_2)HfCH_2C_6H_5$ and the Mechanism of Rearrangement to Its Hafnabenzocyclobutene Tautomer $(\eta^5\text{-}C_5Me_5)_2\overline{HfCH_2\text{-}o\text{-}C}_6H_4$[†]

A. Ray Bulls, William P. Schaefer, Michael Serfas, and John E. Bercaw*

Division of Chemistry and Chemical Engineering, California Institute of Technology, Pasadena, California 91125

Received October 6, 1986

Thermal decomposition of $Cp^*_2Hf(CH_2C_6H_5)_2$ ($Cp^* = \eta^5\text{-}C_5Me_5$) in benzene-$d_6$ cleanly affords toluene and hafnabenzocyclobutene $Cp^*_2\overline{HfCH_2\text{-}o\text{-}C}_6H_4$. Deuterium labeling of the benzyl ligands indicates that decomposition of $Cp^*_2Hf(CY_2C_6H_5)_2$ (Y = H, D) proceeds primarily by α-H abstraction to form a permethylhafnocene benzylidene intermediate $[Cp^*_2Hf{=}CHC_6H_5]$, which rapidly rearranges to the metalated cyclopentadienyl or "tucked-in" benzyl complex $Cp^*(\eta^5,\eta^1\text{-}C_5Me_4CH_2)HfCH_2C_6H_5$. The observed product arises from rearrangement of $Cp^*(\eta^5,\eta^1\text{-}C_5Me_4CH_2)HfCH_2C_6H_5$ to its tautomer $Cp^*_2\overline{HfCH_2\text{-}o\text{-}C}_6H_4$. A series of meta-substituted benzyl derivatives of the proposed metalated cyclopentadienyl intermediates, $Cp^*(\eta^5,\eta^1\text{-}C_5Me_4CH_2)HfCH_2C_6H_4X$ (X = H, CH_3, CF_3, NMe_2), has therefore been prepared. The kinetics of their conversion to $Cp^*_2\overline{HfCH_2\text{-}o\text{-}C}_6H_3X$ have been examined in order to probe the nature of the transition state for aryl C–H bond activation that occurs in the final steps of the rearrangement. The rates are found to be insensitive to the nature of X, suggesting that the benzyl π system is *not* attacked by the electrophilic hafnium center along the reaction coordinate for C–H bond activation. The structure of $Cp^*(\eta^5,\eta^1\text{-}C_5Me_4CH_2)HfCH_2C_6H_5$, as determined by single-crystal X-ray diffraction techniques, indicates that the complex is best described as a Hf(IV) derivative containing an $\eta^5,\eta^1\text{-}C_5Me_4CH_2$ ligand rather than a Hf(II) η^6-fulvene adduct. $Cp^*(\eta^5,\eta^1\text{-}C_5Me_4CH_2)HfCH_2C_6H_5$ crystallizes in the triclinic space group $P\bar{1}$ ($a = 9.084$ (2) Å, $b = 10.492$ (2) Å, $c = 12.328$ (1) Å; $\alpha = 95.81$ (1)°, $\beta = 96.60$ (1)°, $\gamma = 91.15$ (2)°; $Z = 2$). Least-squares refinement led to a value for R of 0.048 ($I > 3\sigma_I$) and a goodness-of-fit of 4.37 for 4029 independent reflections.

Introduction

High-valent, early-transition-metal, lanthanide, and actinide complexes have been shown to be reactive toward both aromatic and aliphatic carbon–hydrogen bonds.[1] Associative mechanisms proceeding through highly ordered, polar, four-centered transition states typically have been invoked for C–H bond cleavage by these d^0 (or d^0f^n) metal systems.[2] An electrophilic aromatic substitution in which the metal interacts initially with the arene π system represents an alternative mechanism for aromatic C–H bond activation.[3] This type of mechanism seems particularly feasible in view of the electron-deficient, highly Lewis acidic nature of coordinatively unsaturated d^0 metal centers. η^3-Coordination of the benzyl ligands of $Zr(OR)(CH_2C_6H_5)_3$ (R = 2,6-di-*tert*-butylphenyl), as evidenced by the X-ray crystal structure, demonstrates such a π-arene–Lewis acid interaction.[4] Similarly, the crystal structures of $Cp^*Th(CH_2C_6H_5)_3$[5] and $M(CH_2C_6H_5)_4$ (M = Ti, Zr, Hf)[6] show the metal to be interacting with the π systems of the benzyl ligands.

There are several examples of transition-metal complexes serving as electrophiles in aromatic substitution reactions. Ogoshi et al. reported arene C–H bond activation by a cationic Rh(III) complex occurred via electrophilic aromatic metalation.[7] Shul'pin and co-workers have invoked a similar mechanism for arene activation at an anionic Pt(IV) center.[8] The intramolecular cyclopalladation of ligands such as azobenzene has also been suggested to occur by electrophilic aromatic substitution, with rearrangement of a π- to σ-arene adduct, followed by loss of a proton leading to the observed aryl product.[9] Deeming and Rothwell, however, have shown that cyclopalladation can also occur with benzo[*h*]quinoline ligands constrained by chelation from forming a π complex.[10] Graham has prepared η^2-arene complexes of the type $[(\eta^5\text{-}C_5H_5)Re(NO)(CO)(\eta^2\text{-arene})]^+$, which closely resemble the proposed intermediates of electrophilic aromatic substitutions.[11] Jones and Feher have developed a convincing

---

[†] Contribution No. 7447.

[1] (a) For a recent review, see: Rothwell, I. P. *Polyhedron* **1985**, *4* (No. 2), 177–200. (b) Thompson, M. E.; Baxter, M. B.; Bulls, A. R.; Burger, B. J.; Nolan, C. N.; Santarsiero, B. D.; Schaefer, W. P.; Bercaw, J. E. *J. Am. Chem. Soc.* **1987**, *109*, 203. (c) Bruno, J. W.; Smith, G. M.; Marks, T. J.; Fair, C. K.; Schultz, A. J.; Williams, J. M. *J. Am. Chem. Soc.* **1986**, *108*, 40.

[2] See, for example: (a) Bruno, J. W.; Marks, T. J.; Day, V. W. *J. Am. Chem. Soc.* **1982**, *104*, 7357–7360. (b) Fagan, P. J.; Manriquez, J. M.; Maatta, E. A.; Seyam, A. M.; Marks, T. J. *J. Am. Chem. Soc.* **1981**, *103*, 6650–6667. (c) Steigerwald, M. L.; Goddard, W. A. *J. Am. Chem. Soc.* **1984**, *106*, 308.

[3] See, for example: (a) Stock, L. *Aromatic Substitution Reactions*, Prentice-Hall: Englewood Cliffs, NJ, 1968. (b) Olah, G. A. *Friedel-Crafts and Related Reactions*, Wiley-Interscience: New York, 1963–1964; Vols. I–IV. (c) Thompson, M. E.; Bercaw, J. E. *Pure Appl. Chem.* **1984**, *56*, 1.

[4] Latesky, S. L.; McMullen, A. K.; Niccolai, G. P.; Rothwell, I. P. Huffman, J. C. *Organometallics*, **1985**, *4*, 902.

[5] Mintz, E. A.; Moloy, K. G., Marks, T. J.; Day, V. W. *J. Am. Chem. Soc.* **1982**, *104*, 4692–4695.

[6] (a) Davies, G. R.; Jarvis, J. A. J.; Kilbourn, B.; Pioli, A. J. P. *J. Chem. Soc., Chem. Commun.* **1971**, 677. (b) Bassi, I. W.; Allegra, G.; Scordamaglia, R.; Chioccola, G. J. *J. Am. Chem. Soc.* **1971**, *93*, 3787–3788. (c) Davies, G. R.; Jarvis, J. A. J.; Kilbourn, B. *J. Chem. Soc., Chem. Commun.* **1971**, 1511–1512.

[7] Aoyama, Y.; Yoshida, T.; Sakurai, K.; Ogoshi, A. *J. Chem. Soc., Chem. Commun.* **1983**, 478.

[8] Shul'pin, G. B.; Nizova, G. V.; Nikitaev, A. T. *J. Organomet. Chem.* **1984**, *276*, 115–153.

[9] (a) Parshall, G. W. *acc. Chem. Res.* **1970**, *3*, 139. (b) Bruce, M. I.; Goodall, B. L.; Stone, F. G. A. *J. Chem. Soc., Chem. Commun.* **1973**, 558.

[10] Deeming, A. J.; Rothwell, I. P. *Pure Appl. Chem.* **1980**, *52*, 649–655.

[11] Sweet, J. R.; Graham, W. A. G. *J. Am. Chem. Soc.* **1983**, *105*, 305–306.

0276-7333/87/2306-1219$01.50/0 © 1987 American Chemical Society

case for the intermediacy of a π-arene adduct along the reaction coordinate leading to C–H bond addition to coordinatively unsaturated $[Cp^*Rh(PMe_3)]$,[12] although this electron-rich rhodium center is not likely to be a strong Lewis acid.

In order to probe the mechanism by which electron-deficient, d^0 metal complexes activate aromatic carbon–hydrogen bonds, we have examined the thermal decomposition of a series of bis(benzyl) derivatives of permethylhafnocene, $Cp^*_2Hf(CH_2C_6H_4\text{-}m\text{-}X)_2$ ($Cp^* = \eta^5\text{-}C_5Me_5$; X = H, CH_3, NMe_2), which cleanly afford toluene (or the substituted toluene) and the hafnobenzocyclobutene complexes $Cp^*_2\overline{HfCH_2\text{-}o\text{-}C_6H_3}X$. Although the most straightforward decomposition pathway to the observed products is direct ortho C–H abstraction from a benzyl ligand by the other $Hf{-}CH_2C_6H_5$ group, a close examination revealed that the mechanism is much more complex; both benzylidene and metalated cyclopentadienyl intermediates are involved. We report herein the synthesis, reactivity, and X-ray structure determination of one intermediate, $Cp^*(\eta^5,\eta^1\text{-}C_5Me_4CH_2)HfCH_2C_6H_5$, and the results of a study of the mechanism of its rearrangement to $Cp^*_2\overline{HfCH_2\text{-}o\text{-}C_6H_4}$.

Results and Discussion

Permethylhafnocene dichloride, $Cp^*_2HfCl_2$ (**1**), reacts rapidly in benzene solution with 2 equiv of the appropriate benzyl potassium reagent[13] to give the dibenzyl complexes **2**–**4** (eq 1). Isolation from petroleum ether affords **2**–**4** in

$$\underset{\mathbf{1}}{Cp^*_2HfCl_2} + 2K(CH_2C_6H_4\text{-}m\text{-}X) \rightarrow Cp^*_2Hf(CH_2C_6H_4\text{-}m\text{-}X)_2 + 2KCl \quad (1)$$

$$\begin{array}{l}\mathbf{2},\ X = H\\ \mathbf{3},\ X = CH_3\\ \mathbf{4},\ X = NMe_2\end{array}$$

good yields as pale yellow crystalline compounds, which may be handled briefly in air and are indefinitely stable at room temperature under an N_2 atmosphere.

Thermolysis of benzene or toluene solutions of **2**–**4** yields the hafnabenzocyclobutenes **5**–**7** and meta-substituted toluene (eq 2).[14] The loss of starting dibenzyl complexes **2**–**4**, monitoring the Cp* peak height vs. an internal ferrocene standard (^{1}H NMR), follows first-order kinetics for 2–3 half-lives.

$$\underset{\mathbf{2-4}}{Cp^*_2Hf(CH_2C_6H_4\text{-}m\text{-}X)_2} \rightarrow Cp^*_2\overline{HfCH_2\text{-}o\text{-}C_6H_3}\text{-}m\text{-}X + CH_3C_6H_4\text{-}m\text{-}X \quad (2)$$

$$\begin{array}{l}\mathbf{5},\ X = H\\ \mathbf{6},\ X = CH_3\\ \mathbf{7},\ X = NMe_2\end{array}$$

Table I. Rates of Decomposition of 2 and 2b–e (Eq 2) and the Isotopically Labeled Toluenes Produced (140 °C, C_6D_6)

compd	$10^{-6}k$, s^{-1}	k_H/k_D	toluene[a]
2	5.81 (19)		$C_6H_5CH_3$
2b	5.29 (27)	1.1 (1)	95% $C_6H_5CH_3$
2c	2.29 (6)	2.5 (2)	80% $C_6D_5CD_3$ 20% $C_6D_5CD_2H$
2d	1.88 (6)	3.1 (2)	85% $C_6H_5CD_3$ 15% $C_6H_5CD_2H$
2e	5.40 (18)	1.1 (1)	95% $C_6D_5CH_3$

[a] Approximate ratio of labeled toluenes were determined by ^{1}H NMR analysis of the product toluene methyl resonance.

Scheme I

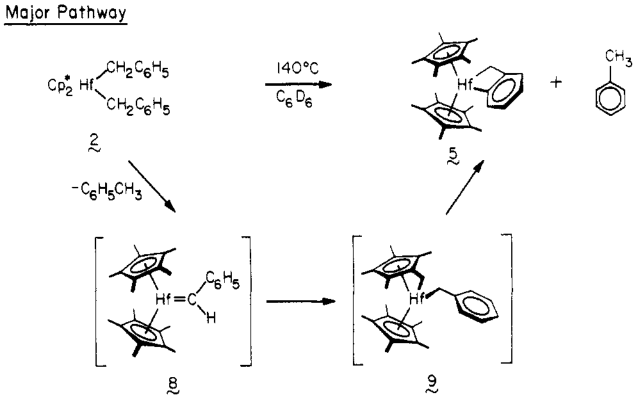

Abstraction of an ortho benzyl hydrogen by the neighboring Hf–benzyl group is the most direct mechanism for the thermal decomposition of **2** to **5**. Hence, we undertook an investigation of the relative rates of decomposition of the meta-substituted dibenzyl complexes **5**–**7** in order to distinguish between an electrophilic aromatic substitution like mechanism, proceeding through an η^1-phenonium ion intermediate or transition state,[15] and a mechanism in which the arene C–H σ bond and Hf–benzyl bonds undergo σ-bond metathesis without interaction of the hafnium center with the arene π system.

To probe whether this straightforward mechanism is, in fact, being followed, the isotopically labeled dibenzyl complexes $(Cp^*\text{-}d_{15})_2Hf(CH_2C_6H_5)_2$ (**2b**), $Cp^*_2Hf(CD_2C_6D_5)_2$ (**2c**), $Cp^*_2Hf(CD_2C_6H_5)_2$ (**2d**), and $Cp^*_2Hf(CH_2C_6D_5)_2$ (**2e**) were prepared as shown in eq 3. Thermal

$$[\eta^5\text{-}C_5(CX_3)_5]_2HfCl_2 + 2KCY_2C_6Z_5 \rightarrow [\eta^5\text{-}C_5(CX_3)_5]_2Hf(CY_2C_6Z_5)_2 + 2KCl \quad (3)$$

$$\begin{array}{l}\mathbf{2},\ X = Y = Z = H\\ \mathbf{2b},\ X = D,\ Y = Z = H\\ \mathbf{2c},\ X = H,\ Y = Z = D\\ \mathbf{2d},\ X = Z = H,\ Y = D\\ \mathbf{2e},\ X = Y = H,\ Z = D\end{array}$$

decomposition of **2e** at 140 °C occurs at roughly the same rate as **2** ($k_H/k_D = 1.07$) and produces ca. 95% $C_6D_5CH_3$[16] (Table I). A moderate deuterium kinetic isotope effect is observed ($k_H/k_D = 3.1$) when the benzyl methylene groups are deuteriated (**2d**), and the toluene produced upon decomposition is approximately 85% $C_6H_5CD_3$. Perdeuteriation of the pentamethylcyclopentadienyl rings (**2b**) results in a small deuterium kinetic isotope effect ($k_H/k_D = 1.1$) and ca. 95% $C_6H_5CH_3$.

The magnitudes of the kinetic deuterium isotope effects and the labeling of the toluene obtained for the thermal decomposition of compounds **2b**–**e** indicate a principal pathway involving a rate-limiting α-H abstraction process (Scheme I) rather than direct transfer of an ortho benzylic hydrogen to the adjacent benzyl group. Particularly indicative of this pathway are the moderate kinetic deuterium isotope effect observed for the decomposition of $Cp^*_2Hf(CY_2C_6H_5)_2$ (Y = H, **2**; Y = D, **2d**), and the formation of toluene-α-d_3 for **2d**. Thus, the hafnium benzy-

---

[12] Jones, W. D.; Feher, F. J. *J. Am. Chem. Soc.* **1984**, *106*, 1650–1663.

[13] Prepared by the dropwise addition of $n\text{-}C_4H_9Li$ to a suspension of $KOCMe_3$ in the appropriately substituted toluene. See: Schlosser, M.; Hartmann, J. *Angew. Chem., Int. Ed. Engl.* **1973**, *12*, 508.

[14] For leading references to related metallacyclobutanes see: (a) Grubbs, R. H. *Comprehensive Organometallic Chemistry*; Wilkinson, G., Stone, F. G. A., Abel, E. W., Eds.; Pergamon: Oxford, 1982; Vol. 8, p 499. (b) Bickelhaupt, F. *Pure Appl. Chem.* **1986**, *58*(4), 537–542. (c) Seetz, J. W. F. L.; Schat, G.; Akkerman, O. S.; Bickelhaupt, F. *Angew. Chem., Int. Engl. Ed.* **1983**, *22*, 248.

[15] Admittedly, the phenonium ion intermediate or transition state for this mechanism would be very strained.

[16] The approximate ratios of isotopically labeled toluenes were determined by integration (^{1}H NMR) of the residual methyl signal.

Table II. Rate Data and Activation Parameters for the Thermal Decomposition of $Cp^*_2Hf(CH_2C_6H_5)_2$ (2) (Benzene-d_6)

T, °C	$10^{-6}k$, s^{-1}	T, °C	$10^{-6}k$, s^{-1}
125	1.11 (5)	140	5.81 (19)
132.5	2.86 (10)	148	14.5 (9)

$\Delta H^* = 34\ (\pm 1)$ kcal/mol
$\Delta S^* = 1\ (\pm 3)$ eu

lidene complex **8** is implicated as an intermediate. Moreover, the observation of deuterium (^2H NMR) in the Cp* ligands of metallacycle product **5** upon thermolysis of $Cp^*_2Hf(CD_2C_6D_5)_2$ (**2c**) suggests the intermediacy of **9**, which could arise from **8** by pentamethylcyclopentadienyl ring hydrogen abstraction. Transfer of an ortho benzylic hydrogen of **9** to the (η^5,η^1-$C_5Me_4CH_2$) ligand finally generates the observed product $Cp^*_2\overline{HfCH_2\text{-}o\text{-}C}_6H_4$ (**5**).

The activation parameters for the thermal decomposition of **2**, over the temperature range 125–148 °C (Table II), $\Delta H^* = 34\ (1)$ kcal mol^{-1} and $\Delta S^* = +1\ (3)$ eu, are similar to those measured for an analogous (rate-limiting) α-hydrogen abstraction process in the thermal decomposition of $Cp^*_2Ti(CH_3)_2$ to $Cp^*(\eta^5,\eta^1\text{-}C_5Me_4CH_2)TiCH_3$ and methane ($\Delta H^* = 27$ kcal mol^{-1} and $\Delta S^* = -2.9$ eu).[17] The conversion of **8** to **9** is similar to that reported by Rothwell et al. for the intramolecular addition of an aliphatic C–H bond across a tantalum–carbon double bond.[18]

The appearance of ca. 20% $C_6D_5CD_2H$ from the thermolysis of $Cp^*_2Hf(CD_2C_6D_5)_2$ (**2c**) in benzene-d_6 indicates that direct abstraction of a pentamethylcyclopentadienyl ring hydrogen by a departing hafnium benzyl ligand, generating intermediate **9** without the intermediacy of **8**, is a competitive pathway for the decomposition of $Cp^*_2Hf(CH_2C_6H_5)_2$. This minor pathway is likely to be most prominent when the α-hydrogen abstraction is slowed by deuteriation of the benzyl methylene groups as in **2c** and **2d**. Also consistent with direct pentamethylcyclopentadienyl ring hydrogen abstraction being a relatively minor pathway is the small deuterium kinetic isotope effect observed upon the thermolysis of $(Cp^*\text{-}d_{15})_2Hf(CH_2C_6H_5)_2$ (**2b**).

The proposed intermediate **9** and its meta-substituted analogues **13–15** can be prepared independently in high yields by the route shown in eq 4–6. A moderate deuterium kinetic isotope effect (k_H/k_D at 140 °C = 3.75) is observed upon thermolysis of $(Cp^*\text{-}d_{15})_2Hf(CH_2CMe_3)I$, suggesting that formation of $Cp^*(\eta^5,\eta^1\text{-}C_5Me_4CH_2)HfI$ proceeds by the rate-limiting coupling of the neopentyl ligand and a pentamethylcyclopentadienyl ring hydrogen.

$$Cp^*_2HfI_2 + LiCH_2CMe_3 \rightarrow Cp^*_2Hf(CH_2CMe_3)I + Li^+I^- \quad (4)$$

$$Cp^*_2Hf(CH_2CMe_3)I \xrightarrow{140\ ^\circ C} Cp^*(\eta^5,\eta^1\text{-}C_5Me_4CH_2)HfI + C(CH_3)_4 \quad (5)$$

$$Cp^*(\eta^5,\eta^1\text{-}C_5Me_4CH_2)HfI + MCH_2C_6H_4\text{-}m\text{-}X \rightarrow M^+I^- + Cp^*(\eta^5,\eta^1\text{-}C_5Me_4CH_2)Hf(CH_2C_6H_4\text{-}m\text{-}X) \quad (6)$$

9, X = H
13, X = CH_3
14, X = CF_3
15, X = NMe_2

M = K or MgCl

In benzene solution compounds **9** and **13–15** readily rearrange to hafnabenzocyclobutenes **5–7** and **16**, but unlike the thermally robust dibenzyl complexes **2–4**, this conversion occurs slowly over several days at room temperature (eq 7). The lack of reactivity of the pentamethylcyclopentadienyl-metalated iodide derivative $Cp^*(\eta^5,\eta^1\text{-}C_5Me_4CH_2)HfI$ toward benzene (and benzene-d_6) solvent, even on prolonged heating at 140 °C, is striking evidence of the tremendous kinetic advantage that *intramolecular* C–H bond activation has over *intermolecular* C–H activation for these sterically encumbered permethylhafnocene derivatives.[19]

$$\underset{\mathbf{9,\ 13\text{–}15}}{Cp^*(\eta^5,\eta^1\text{-}C_5Me_4CH_2)Hf(CH_2C_6H_4\text{-}m\text{-}X)} \rightarrow Cp^*_2\overline{HfCH_2\text{-}o\text{-}C}_6H_3\text{-}m\text{-}X \quad (7)$$

5, X = H
6, X = CH_3
7, X= NMe_2
16, X = CF_3

$Cp^*(\eta^5,\eta^1\text{-}C_5Me_4CH_2)HfCD_2C_6D_5$ (**9**-d_7), obtained by treating $Cp^*(\eta^5,\eta^1\text{-}C_5Me_4CH_2)HfI$ with (benzyl-d_7)potassium, decomposes much more slowly than $Cp^*(\eta^5,\eta^1\text{-}C_5Me_4CH_2)HfCH_2C_6H_5$ ($k_H/k_D = 9.6$ at 59 °C), consistent with benzylic C–H or C–D bond cleavage in the rate-determining step. Deuterium is observed in the pentamethylcyclopentadienyl ligand (^2H NMR) of the hafnabenzocyclobutene **5**-d_7 derived from **9**-d_7. Steric factors should favor activation of the benzylic hydrogen that is para rather than ortho to the substituent X in **13–15**, and high-field ^1H NMR spectra (400 MHz) of **6**, **7**, and **16** indicate X is, indeed, para to hafnium (Table III). Moreover, the rate of conversion of **9** (X = H) to metallacycle **5** is roughly twice that measured for the conversion of **13–15** to metallacycles **6**, **7**, and **16**, since the concentration of reactive (sterically unencumbered) C–H bonds for **9** is twice that of the compounds where X $\neq$ H.

Kinetic data and activation parameters for the rearrangement of the cyclopentadienyl-metalated benzyl derivatives **9** and **13–15** to the corresponding metallacycles **5–7** and **16** are given in Table IV. As can be seen, the rates of decomposition are nearly independent of the nature of X, and a plot of log k (at 32 °C) vs. the Hammett constants σ_{para}[20] gives a reasonably linear fit with $\rho = -0.2$.[21] Whereas the sign of ρ is in agreement with an electrophilic aromatic substitution mechanism, its small value argues against this pathway for the decomposition of **9** and **13–15**, in spite of the electrophilic nature of the hafnium center. Values of ρ for electrophilic aromatic substitution by cationic organic and inorganic electrophiles typically range from −1.5 to −12.[22] Unfavorable steric interactions between the benzyl ligand and the two pentamethylcyclopentadienyl ligands likely prevent the arene from coordinating to the hafnium center with its π system aligned with the vacant orbital on the permethylhafnocene moiety, as would be required for an electrophilic aromatic substitution mechanism. Similar, unfavorable steric interactions were invoked to reconcile the noninvolvement of

---

[17] McDade, C.; Green, J. C.; Bercaw, J. E. *Organometallics* **1982**, *1*, 1629.

[18] Chamberlain, L.; Rothwell, I. P.; Huffman, J. C. *J. Am. Chem. Soc.* **1982**, *104*, 7338–7340.

[19] $(\eta^5\text{-}C_5Me_5)_2Hf(C_6H_5)I$ does not liberate C_6H_6 (to generate **12**) when thermolyzed (140 °C) for 4 days in C_6D_6. Furthermore, deuterium is not incorporated (^2H NMR) into **12** when heated for extended periods in C_6D_6.

[20] Johnson, C. D. *The Hammett Equation*; Cambridge University Press: Cambridge, 1973.

[21] For the purpose of constructing a Hammett plot, the rate constant for **9** (X = H) rearranging to **5** was corrected for having two kinetically available ortho benzyl hydrogens; i.e., the value of k (X = H) was halved.

[22] Lowry, T. H.; Richardson, K. S. *Mechanism and Theory in Organic Chemistry*; Wasserman, M.; Castellano, E., Eds.; Harper & Row: New York, 1981; pp 559–580.

Scheme II

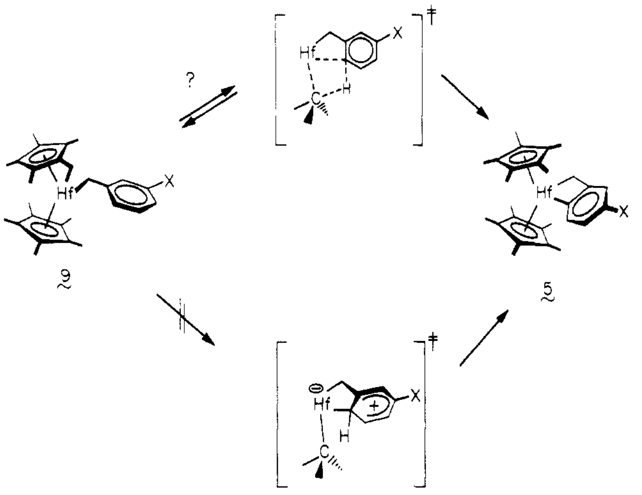

Scheme III

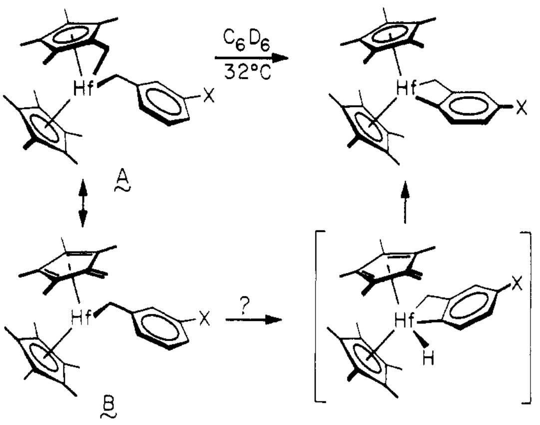

the π system in "σ-bond metathesis" reactions between (η^5-C_5Me_5)$_2$Sc–CH_3 and substituted arenes C_6H_5X (X = CF_3, H, CH_3, OCH_3, NMe_2) to yield (η^5-C_5Me_5)$_2$Sc–C_6H_4X and methane.[1b] Moreover, models suggest considerable ring strain accompanies the transition state for the lower pathway of Scheme II. Thus, the mechanism for conversion of Cp*(η^5,η^1-$C_5Me_4CH_2$)Hf–$CH_2C_6H_5$ to $Cp^*_2\overline{HfCH_2\text{-}o\text{-}C}_6H_4$ appears to involve attack of hafnium at an ortho benzylic C–H bond with the phenyl ring roughly parallel to the metalated cyclopentadienyl ligands (upper pathway of Scheme III).

The very small substituent effects for aryl C–H bond activation observed for both permethylscandocene and permethylhafnocene alkyls would appear to indicate similar mechanisms. σ-Bond metathesis involving d^0 (η^5-C_5Me_5)$_2$Sc–R derivatives almost certainly proceeds via a four-centered, nonredox mechanism, and such reactions of permethylhafnocene alkyls may well proceed by the same. On the other hand, an oxidative addition/reductive elimination sequence (lower pathway, Scheme III) must be considered for the cyclopentadienyl-metalated hafnium derivatives **9** and **13–15**, since two limiting resonance forms, Cp*(η^5,η^1-$C_5Me_4CH_2$)Hf^{IV}($CH_2C_6H_4$-*m*-X) (A) and Cp*(η^6-$C_5Me_4CH_2$)Hf^{II}($CH_2C_6H_4$-*m*-X) (B), describe them. Thus, a distinction between mechanisms (upper pathway of Scheme II or lower pathway of Scheme III) rests on which of the two limiting resonance forms (A or B) best describes the ground states of **9** and **13–15**.

NMR data suggest the structure of **9** is intermediate between resonance forms A and B. The diastereotopic hydrogens of the bridging methylene are coupled to each other with $^2J_{HH}$ = 8.5 Hz, intermediate between typical values for geminal sp^2 and sp^3 hydrogens of 0–3 and 12–15 Hz, respectively. The gated (^{1}H NOE-enhanced) carbon spectrum for **9** exhibits a signal for the methylene carbon at δ 71.2 with $^1J_{CH}$ = 142 Hz, again intermediate between $^1J_{CH}$ values for sp^2 and sp^3 of 125 and 160 Hz, respectively.

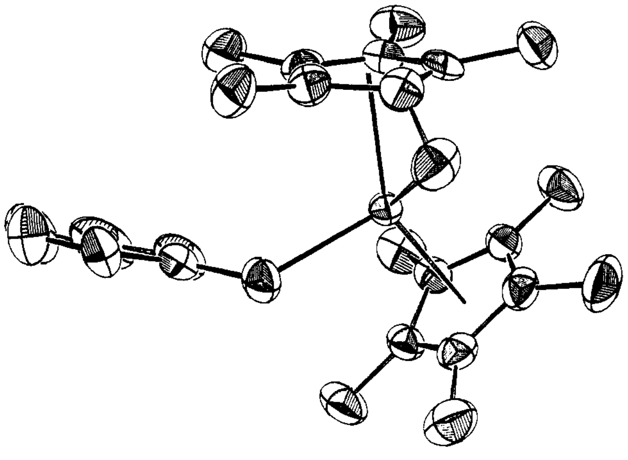

Figure 1. Molecular configuration of **9**. Thermal ellipsoids are shown at the 50% probability level.

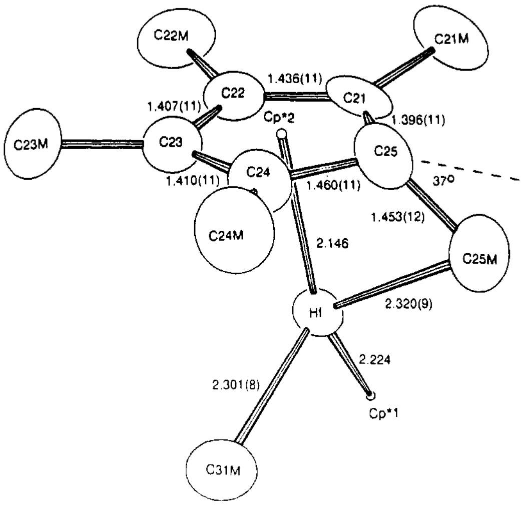

Figure 2. Skeletal view of **9**.

In view of the ambiguities in these NMR data, an *x*-ray crystal structure determination was undertaken in hopes of distinguishing between A and B. The molecular structure of **9** is shown in Figure 1, and a skeletal view is shown in Figure 2. Unlike the unmetalated (η^5-C_5Me_5) ring, which has ring C–C distances from 1.414 (10) to 1.424 (11) Å, the metalated (η^5-C_5Me_5) C–C distances vary from 1.396 (11) to 1.460 (11) Å. The variations are *not* indicative of an η^6-fulvene ligand, however. For example, the three carbon–carbon single bonds in the η^6-fulvene formalism average 1.421 (11) Å, whereas the two internal carbon–carbon double bonds are insignificantly longer (averaging 1.423 (11) Å). The C25M–Hf distance (2.320 (9) Å) is only 0.06 Å longer than the C25–Hf distance of 2.258 (8) Å, and C25M is bent (an impressive) 37° out of the ring carbon plane toward Hf. The C25–C25M distance is 1.453 (12) Å is somewhat shorter (0.046 Å) than the average ring carbon to methyl carbon distance of 1.499 (11) Å.

Few compounds containing a coordinated fulvene ligand have been structurally characterized for comparison to Cp*(η^5,η^1-$C_5Me_4CH_2$)$HfCH_2C_6H_5$.[23] Green and co-workers

---

[23] Following submission of this manuscript, a closely related "σ,η^5-$C_5Me_4CH_2$" derivative has been described. Schock, L. E.; Brock, C. P.; Marks, T. J. *Organometallics* 1987, *6*, 232.

reported a series of fulvene complexes of the type M(η^5,η^1-$C_5H_4CR_2$)(η^6-C_6H_5R') (M = Mo or W; R = CH_3 or C_6H_5; R′ = H or CH_3) along with the titanium complex Ti(η^5,η^1-$C_5H_4CPh_2$)$_2$.[24] On the basis of ring carbon to methylene carbon distances of 1.42(2)–1.45(3) Å and values of θ[25] ranging from 36 to 39°, these authors concluded the metal–fulvene moiety is better described as M^{II}(η^5,η^1-$C_5H_4CR_2$) than as M^0(η^6-$C_5H_4CR_2$). The similar structural features found for the tetramethylfulvene moiety for Cp*(η^5,η^1-$C_5Me_4CH_2$)$HfCH_2C_6H_5$ would, by extension of Green's reasoning, argue for Cp*(η^5,η^1-$C_5Me_4CH_2$)Hf^{IV}($CH_2C_6H_4$-*m*-X) (resonance form A) structures for **9** and **13**–**15**.[26]

Conclusions

Labeling experiments demonstrate that the thermal decomposition of $Cp^*_2Hf(CH_2C_6H_5)_2$ (**2**) occurs primarily by an α-H abstraction process to generate a transient hafnium benzylidene species, which rearranges to the metalated cyclopentadienyl benzyl complex Cp*(η^5,η^1-$C_5Me_4CH_2$)$HfCH_2C_6H_5$ (**9**) and finally to the observed hafnabenzocyclobutene $Cp^*_2\overline{HfCH_2\text{-}o\text{-}C}_6H_4$ (**5**). A convenient starting material for the synthesis of a series of metalated cyclopentadienyl derivatives of permethylhafnocene is Cp*(η^5,η^1-$C_5Me_4CH_2$)HfI, obtained in high yield by the pyrolysis of $Cp^*_2Hf(CH_2CMe_3)I$. The small rate differences among the series of complexes Cp*(η^5,η^1-$C_5Me_4CH_2$)Hf($CH_2C_6H_4$-*m*-X) (X = CF_3, H, CH_3, NMe_2) and the relatively large negative values for the activation entropies indicate that the thermal rearrangement of Cp*(η^5,η^1-$C_5Me_4CH_2$)$HfCH_2C_6H_5$ to $Cp^*_2\overline{HfCH_2\text{-}o\text{-}C}_6H_4$ occurs by a highly ordered, four-centered transition state, similar to that observed for intermolecular, σ-bond metathesis reactions involving arenes and permethylscandocene alkyls.[1b] Specifically, the cleavage of the aryl C–H bond occurs by direct attack of the electrophilic hafnium center at the carbon–hydrogen σ bond, without interaction of the π orbitals of the arene (i.e. according to the upper pathway of Scheme II).

Experimental Section

General Considerations. All manipulations were performed by using glovebox or high vacuum techniques. Solvents were purified by distillation from Na metal under an N_2 atmosphere followed by vacuum transfer from "titanocene". NMR solvents were purified by vacuum transfer from activated molecular sieves (4 Å, Linde) and then from "titanocene". ^1H, ^2H, and ^{13}C NMR spectra were obtained by using Varian EM-390 (90 MHz, ^1H) and JEOL GX400Q (400 MHz, ^1H; 100 MHz, ^{13}C; 60.4 MHz, ^2H) spectrometers. Elemental analyses were performed by Larry Henling of the CIT Analytical Laboratory.

Procedures. $\mathbf{Cp^*_2Hf(CH_2C_6H_5)_2}$ **(2).** Permethylhafnocene dichloride **1** (1.40 g, 2.70 mmol) and $KCH_2C_6H_5$ (0.95 g, 7.31 mmol) were stirred overnight in 20 mL of benzene. Following filtration the benzene was replaced with 10 mL of petroleum ether. Cooling to −78 °C and filtering yielded 0.90 g (52%) of yellow **2**. Anal. Calcd for $HfC_{34}H_{44}$: C, 64.73; H, 6.97. Found: C, 64.93; H, 6.85. The isotopically labeled bis(benzyl) compounds **2b**–**e** were prepared in an analogous manner from the appropriately labeled starting materials.

Preparation of $\mathbf{(Cp^*\text{-}d_{15})_2HfI_2}$**.** To a large glass bomb was added $Cp^*_2HfH_2$ (0.46 g, 1.0 mmol) and ca. 10 mL of benzene-d_6. Deuterium gas admitted into the apparatus at −196 °C. This solution was heated to 115 °C with stirring for 5 days. The bomb was recharged daily with fresh deuterium gas. At the end of 5 days excess CH_3I was condensed into the bomb resulting in the rapid formation of $(Cp^*\text{-}d_{15})_2HfI_2$, which was isolated from petroleum ether (0.39 g, 55%). The total isotopic purity was ≥95% (^1H NMR).

$\mathbf{Cp^*_2Hf(CH_2C_6H_4\text{-}}$***m***$\mathbf{\text{-}CH_3)_2}$ **(3).** The diiodide derivative $Cp^*_2HfI_2$ (1.07 g, 1.52 mmol) and $KCH_2C_6H_4$-*m*-CH_3 (0.69 g, 4.79 mmol) were stirred overnight in ca. 20 mL of benzene. After the solution was filtered, the benzene was replaced with ca. 10 mL of petroleum ether. Cooling to −78 °C and filtering yielded 0.48 g (48%) of pale yellow **3**. Anal. Calcd for $HfC_{36}H_{48}$: C, 65.59; H, 7.34. Found: C, 66.31; H, 7.54.

$\mathbf{Cp^*_2Hf(CH_2C_6H_4\text{-}}$***m***$\mathbf{\text{-}NMe_2)_2}$ **(4).** Compound **1** (1.67 g, 3.21 mmol) and 1.4 (8.09 mmol) of $KCH_2C_6H_4$-*m*-NMe_2 were stirred overnight in ca. 20 mL of benzene. After the solution was filtered, the benzene was replaced with ca. 10 mL of petroleum ether. Cooling to −78 °C and filtering yielded 1.75 g (71%) of pale yellow **4**. Anal. Calcd for $HfC_{38}H_{54}N_2$: C, 63.57; H, 7.66; N, 3.90. Found: C, 63.84; H, 7.52; N, 3.92.

$\mathbf{Cp^*_2\overline{HfCH_2\text{-}}}$$\overline{\boldsymbol{o}\mathbf{\text{-}C}}$$\mathbf{_6H_4}$ **(5).** To a small glass bomb was added 1.17 g (1.85 mmol) of **2** and ca. 10 mL of methylcyclohexane. The solution was heated to 140 °C for 6 days. Isolation from petroleum ether yielded 0.61 g of pale yellow **5** (61%). Anal. Calcd for $HfC_{27}H_{36}$: C, 60.62; Hf, 6.77. Found: C, 60.86; H, 6.84.

$\mathbf{Cp^*_2\overline{HfCH_2\text{-}}}$$\overline{\boldsymbol{o}\mathbf{\text{-}C}}$$\mathbf{_6H_3\text{-}}$***m***$\mathbf{\text{-}NMe_2}$ **(7).** To a small glass bomb was added compound **4** (0.75 g, 1.0 mmol) and 5 mL of toluene. This solution was heated for 2 days at 145 °C. Isolation from −78 °C petroleum ether afforded 0.18 g of pale yellow **7** (30%). Anal. Calcd for $HfC_{29}H_{41}N$: C, 59.83; H, 7.10; N, 2.41. Found: C, 59.31; H, 7.37; N, 2.23.

$\mathbf{Cp^*(\eta^5,\eta^1\text{-}C_5Me_4CH_2)HfCH_2C_6H_5}$ **(9).** Cp*(η^5,η^1-$C_5Me_4CH_2$)HfI (0.82 g, 1.4 mmol) and $KCH_2C_6H_5$ (0.19 g, 1.5 mmol) were stirred for 1 h in 10 mL of benzene. After the solution was filtered, the benzene was replaced with 10 mL of petroleum ether. Cooling to −78 °C and filtering yielded 0.42 g (52%) of yellow-orange **9**. Anal. Calcd for $HfC_{27}H_{36}$: C, 60.16; H, 6.73. Found: C, 60.47; H, 6.74.

$\mathbf{Cp^*_2Hf(CH_2CMe_3)I}$ **(11).** Permethylhafnocene diiodide (0.94 g, 1.5 mmol) and $LiCH_2CMe_3$ (0.13 g, 1.6 mmol) were stirred overnight in benzene. Following filtration the benzene was replaced with 10 mL of petroleum ether. Cooling to −78 °C and filtering afforded 0.74 g (85%) of yellow $Cp^*_2Hf(CH_2CMe_3)I$. Anal. Calcd for $HfC_{25}H_4I$: C, 46.44; H, 6.39. Found: C, 46.15; H, 6.16.

$\mathbf{Cp^*(\eta^5,\eta^1\text{-}C_5Me_4CH_2)HfI}$ **(12).** To a small glass bomb was added $Cp^*_2Hf(CH_2CMe_3)I$ (4.24 g, 6.54 mmol) and 30 mL of toluene. This solution was heated at 140 °C for 2 days. Isolation from petroleum ether at −78 °C yielded 2.1 g (56%) of orange Cp*(η^5,η^1-$C_5Me_4CH_2$)Hfi. Anal. Calcd for $HfC_{20}H_{29}I$: C, 41.79; H, 5.08. Found: C, 42.27; H, 5.07.

$\mathbf{Cp^*(\eta^5,\eta^1\text{-}C_5Me_4CH_2)Hf(CH_2C_6H_4\text{-}}$***m***$\mathbf{\text{-}CH_3)}$ **(13).** Cp*(η^5,η^1-$C_5Me_4CH_2$)HfI (0.90 g, 1.6 mmol) and $KCH_2C_6H_4$-*m*-CH_3 (0.33 g, 2.29 mmol) were stirred for 1 h in 20 mL of benzene. Following filtration the benzene was replaced with 5 mL of petroleum ether. Cooling to −78 °C and filtering yielded 0.50 g (56%) of yellow-orange **10**. Anal. Calcd for $HfC_{28}H_{38}$: C, 60.84; H, 6.87. Found: C, 58.80; H, 6.65.

$\mathbf{Cp^*(\eta^5,\eta^1\text{-}C_5Me_4CH_2)Hf(CH_2C_6H_4\text{-}}$***m***$\mathbf{\text{-}CF_3)}$ **(14).** Cp*(η^5,η^1-$C_5Me_4CH_2$)HfI (0.75 g, 1.30 mmol) and 1.1 equiv of $ClMgCH_2C_6H_4$-*m*-CF_3 were stirred in 10 mL of diethyl ether for 1 h. The solvent was replaced with petroleum ether, and the solution was filtered. Cooling to −78 °C and filtering yielded 0.57 g (72%) of yellow-orange **11**. Anal. Calcd for $HfC_{28}H_{35}F_3$: C, 55.31; H, 5.97. Found: C, 54.49; H, 5.77.

$\mathbf{Cp^*(\eta^5,\eta^1\text{-}C_5Me_4CH_2)Hf(CH_2C_6H_4\text{-}}$***m***$\mathbf{\text{-},NMe_2)}$ **(15).** Cp*(η^5,η^1-$C_5Me_4CH_2$)HfI (0.81 g, 1.4 mmol) and $KCH_2C_6H_4$-*m*-NMe_2 (0.25 g, 1.46 mmol) were stirred for 1 h in 10 mL of benzene. After the solution was filtered, the solvent was replaced with petroleum ether. Cooling to −78 °C and then filtering afforded 0.37 g (45%)

---

[24] Bandy, J. A.; Mtetwa, V. S. B.; Prout, K.; Green, J. C.; Davies, C. E.; Green, M. L. H.; Hazel, N. J.; Izquierdo, A.; Martin-Polo, J. J. *J. Chem. Soc. Dalton Trans.* **1985**, 2037 and references therein.

[25] θ is defined as the angle by which the exocyclic bond of the fulvene ligand deviates from planarity with the five ring carbons of the cyclopentadienyl ligand. This deviation is toward the metal center.

[26] There are no indications of interaction between the hafnium and the aryl ring of the benzyl ligand (i.e. an η^3-$CH_2C_6H_5$ interaction) for **9**, in contrast to the structures of other, analogous benzyl complexes (vida supra).

Table III. ^{1}H and ^{13}C NMR Data[a]

compound	assign	δ[b]	coupling[c]
$\mathrm{Cp^*_2Hf(CH_2C_6H_5)_2}$ (**2**)	$\eta^5\text{-}\mathrm{C_5(\mathit{CH}_3)_5}$	1.77 s	
	$\mathrm{\mathit{CH}_2C_6H_5}$	1.41 br	
	$\mathrm{CH_2C_6\mathit{H}_5}$	6.83–7.33 m	
$\mathrm{Cp^*_2Hf(CH_2C_6H_4\text{-}\mathit{m}\text{-}CH_3)_2}$ (**3**)	$\eta^5\text{-}\mathrm{C_5(\mathit{CH}_3)_5}$	1.78 s	
	$\mathrm{\mathit{CH}_2C_6H_4CH_3}$	1.44 br	
	$\mathrm{CH_2C_6H_4\mathit{CH}_3}$	2.27 s	
	$\mathrm{CH_2C_6\mathit{H}_4CH_3}$	6.73–7.27 m	
$\mathrm{Cp^*_2Hf(CH_2C_6H_4\text{-}\mathit{m}\text{-}NMe_2)_2}$ (**4**)	$\eta^5\text{-}\mathrm{C_5(\mathit{CH}_3)_5}$	1.83 s	
	$\mathrm{\mathit{CH}_2C_6H_4NMe_2}$	1.50 br	
	$\mathrm{CH_2C_6\mathit{H}_4NMe_2}$	6.37–7.30 m	
	$\mathrm{CH_2C_6H_4N(\mathit{CH}_3)_2}$	2.71 s	
$\mathrm{Cp^*_2\overline{HfCH_2\text{-}\mathit{o}\text{-}C}_6H_4}$ (**5**)	$\eta^5\text{-}\mathrm{C_5(\mathit{CH}_3)_5}$	1.68 s	
	$\mathrm{\mathit{CH}_2C_6H_4}$	2.30 br	
	$\mathrm{CH_2C_6\mathit{H}_4}$	7.03–7.80 m	
$\mathrm{Cp^*_2\overline{HfCH_2\text{-}\mathit{o}\text{-}C}_6H_3\text{-}\mathit{m}\text{-}Me}$ (**6**)	$\eta^5\text{-}\mathrm{C_5(\mathit{CH}_3)_5}$	1.62 s	
	$\mathrm{\mathit{CH}_2C_6H_3CH_3}$	2.13 br	
	$\mathrm{CH_2C_6\mathit{H}_3CH_3}$	7.52 s	
		7.44 d	$^3J_{\mathrm{HH}} = 7.0$
		7.10 d	$^3J_{\mathrm{HH}} = 7.0$
	$\mathrm{CH_2C_6H_3\mathit{CH}_3}$	2.16 s	
$\mathrm{Cp^*_2\overline{HfCH_2\text{-}\mathit{o}\text{-}C}_6H_3\text{-}\mathit{m}\text{-}NMe_2}$ (**7**)	$\eta^5\text{-}\mathrm{C_5(\mathit{CH}_3)_5}$	1.75 s	
	$\mathrm{\mathit{CH}_2C_6H_3NMe_2}$	2.37 br	
	$\mathrm{CH_2C_6\mathit{H}_3NMe_2}$	7.48 d	$^3J_{\mathrm{HH}} = 7.6$
		7.18 d	$^4J_{\mathrm{HH}} = 2.2$
		6.81 dd	$^3J_{\mathrm{HH}} = 7.6$
			$^4J_{\mathrm{HH}} = 2.2$
	$\mathrm{CH_2C_6H_3N(\mathit{CH}_3)_2}$	2.72 s	
$\mathrm{Cp^*(\eta^5,\eta^1\text{-}C_5Me_4CH_2)Hf(CH_2C_6H_5)}$ (**9**)	$\eta^5\text{-}\mathrm{C_5(\mathit{CH}_3)_5}$	1.88 s	
	$\mathrm{C_5(CH_3)_4\mathit{CH}_2}$	1.54 d	$^2J_{\mathrm{HH}} = 7.6$
		1.96 d	$^2J_{\mathrm{HH}} = 7.6$
	$\mathrm{C_5(\mathit{CH}_3)_4CH_2}$	1.43 s	
		1.52 s	
		1.67 s	
		1.95 s	
	$\mathrm{\mathit{CH}_2C_6H_5}$	−0.33 d	$^2J_{\mathrm{HH}} = 14.4$
		2.13 d	$^2J_{\mathrm{HH}} = 14.4$
	$\mathrm{CH_2C_6\mathit{H}_5}$	6.85–7.15 m	
	$\mathrm{\mathit{C}H_2C_6H_5}$	57.25 t	$^1J_{\mathrm{CH}} = 113$
	$\eta^5\text{-}\mathrm{C_5(\mathit{C}H_3)_5}$	12.19 q	$^1J_{\mathrm{CH}} = 125$
	$\eta^5\text{-}\mathrm{\mathit{C}_5(CH_3)_5}$	117.5 s	
	$\mathrm{C_5(CH_3)_4\mathit{C}H_2}$	71.24 t	$^1J_{\mathrm{CH}} = 142$
$\mathrm{Cp^*_2Hf(CH_2CMe_3)I}$ (**11**)	$\eta^5\text{-}\mathrm{C_5(\mathit{CH}_3)_5}$	2.00 s	
	$\mathrm{\mathit{CH}_2C(CH_3)_3}$	0.02 s	
	$\mathrm{CH_2C(\mathit{CH}_3)_3}$	1.27 s	
$\mathrm{Cp^*(\eta^5,\eta^1\text{-}C_5Me_4CH_2)HfI}$ (**12**)	$\eta^5\text{-}\mathrm{C_5(CH_3)_5}$	1.96 s	
	$\mathrm{C_5(CH_3)_4\mathit{CH}_2}$	1.42 d	$^2J_{\mathrm{HH}} = 7.8$
		1.99 d	$^2J_{\mathrm{HH}} = 7.8$
	$\mathrm{C_5(\mathit{CH}_3)_4CH_2}$	1.53 s	
		1.69 s	
		1.98 s	
		2.40 s	
	$\eta^5\text{-}\mathrm{C_5(\mathit{C}H_3)_5}$	13.22 q	$^1J_{\mathrm{CH}} = 126$
	$\eta^5\text{-}\mathrm{\mathit{C}_5(CH_3)_5}$	118.91 s	
	$\mathrm{C_5(CH_3)_4\mathit{C}H_2}$	74.9 t	$^1J_{\mathrm{CH}} = 144$
$\mathrm{Cp^*(\eta^5,\eta^1\text{-}C_5Me_4CH_2)Hf(CH_2C_6H_4\text{-}\mathit{m}\text{-}CH_3)}$ (**13**)	$\eta^5\text{-}\mathrm{C_5(\mathit{CH}_3)_5}$	1.90 s	
	$\mathrm{C_5(CH_3)_4\mathit{CH}_2}$	1.55 d	$^2J_{\mathrm{HH}} = 7.5$
		1.88 d	$^2J_{\mathrm{HH}} = 7.5$
	$\mathrm{C_5(\mathit{CH}_3)_4CH_2}$	1.44 s	
		1.55 s	
		1.69 s	
		1.96 s	
	$\mathrm{\mathit{CH}_2C_6H_4CH_3}$	−0.30 d	$^2J_{\mathrm{HH}} = 13.8$
		1.91 s	$^2J_{\mathrm{HH}} = 13.8$
	$\mathrm{CH_2C_6H_4\mathit{CH}_3}$	2.22 s	
	$\mathrm{CH_2C_6\mathit{H}_4CH_3}$	6.43–7.07 m	
	$\mathrm{\mathit{C}H_2C_6H_4CH_3}$	56.93 t	$^1J_{\mathrm{CH}} = 113$
	$\eta^5\text{-}\mathrm{C_5(\mathit{C}H_3)_5}$	12.22 q	$^1J_{\mathrm{CH}} = 125$
	$\eta^5\text{-}\mathrm{\mathit{C}_5(CH_3)_5}$	117.49 s	
	$\mathrm{C_5(CH_3)_4\mathit{C}H_2}$	71.09 t	$^1J_{\mathrm{CH}} = 142$
$\mathrm{Cp^*(\eta^5,\eta^1\text{-}C_5Me_4CH_2)Hf(CH_2C_6H_4\text{-}\mathit{m}\text{-}CF_3)}$ (**14**)	$\eta^5\text{-}\mathrm{C_5(\mathit{CH}_3)_5}$	1.84 s	
	$\mathrm{C_5(CH_3)_4\mathit{CH}_2}$	1.50 d	$^2J_{\mathrm{HH}} = 7.6$
		1.89 d	$^2J_{\mathrm{HH}} = 7.6$
	$\mathrm{C_5(\mathit{CH}_3)_4CH_2}$	1.28 s	
		1.47 s	
		1.61 s	

Table III (Continued)

compound	assignt	δ^b	coupling^c
		1.83 s	
	$C\mathit{H}_2C_6H_4CF_3$	−0.45 d	$^2J_{HH}$ = 14.0
		1.87 d	$^2J_{HH}$ = 14.0
	$CH_2C_6\mathit{H}_4CF_3$	6.80–7.12 m	
	$\eta^5\text{-}C_5(\mathit{C}H_3)_5$	12.10 q	$^1J_{CH}$ = 125
	$\eta^5\text{-}C_5(CH_3)_5$	117.78 s	
	$\mathit{C}H_2C_6H_4CF_3$	55.93 t	$^1J_{CH}$ = 113
	$C_5(CH_3)_4\mathit{C}H_2$	71.51 t	$^1J_{CH}$ = 142
$Cp^*(\eta^5,\eta^1\text{-}C_5Me_4CH_2)Hf(CH_2C_6H_4\text{-}m\text{-}NMe_2)$ (**15**)	$\eta^5\text{-}C_5(C\mathit{H}_3)_5$	1.91 s	
	$C_5(CH_3)_4C\mathit{H}_2$	1.58 d	$^2J_{HH}$ = 7.5
		2.03 d	$^2J_{HH}$ = 7.5
	$C_5(C\mathit{H}_3)_4CH_2$	1.53 s	
		1.55 s	
		1.68 s	
		2.04 s	
	$CH_2C_6H_4N(C\mathit{H}_3)_2$	2.67 s	
	$C\mathit{H}_2C_6H_4N(CH_3)_2$	−0.30 d	$^2J_{HH}$ = 14.0
		2.13 d	$^2J_{HH}$ = 14.0
	$CH_2C_6\mathit{H}_4N(CH_3)_2$	6.15–7.10 m	
	$\eta^5\text{-}C_5(\mathit{C}H_3)_5$	12.24 q	$^1J_{CH}$ = 125
	$\eta^5\text{-}\mathit{C}_5(CH_3)_5$	117.45 s	
	$\mathit{C}H_2C_6H_4N(CH_3)_2$	57.82 t	$^1J_{CH}$ = 113
	$C_5(CH_3)_4\mathit{C}H_2$	71.12 t	$^1J_{CH}$ = 142
$Cp^*{}_2\overline{HfCH_2\text{-}o\text{-}C}_6H_3\text{-}m\text{-}CF_3$ (**16**)	$\eta^5\text{-}C_5(C\mathit{H}_3)_5$	1.54 s	
	$C\mathit{H}_2C_6H_3CF_3$	2.03 br	
	$CH_2C_6\mathit{H}_3CF_3$	7.87 s	
		7.46 d	$^3J_{HH}$ = 7.3
		7.34 d	$^3J_{HH}$ = 7.3

[a] NMR spectra were recorded in benzene-d_6 at ambient temperature. [b] Chemical shifts are reported in parts per million (δ) from tetramethylsilane. [c] Coupling constants are reported in hertz.

Table IV. Rate Constants and Activation Parameters for the Thermal Conversion of $Cp^*(\eta^5,\eta^1\text{-}C_5Me_4CH_2)Hf(CH_2C_6H_4\text{-}m\text{-}X)$ to 5–7 and 16 (Benzene-d_6)

X	T, °C	$10^{-6}k$, s^{-1}	$\Delta H^\ddagger$, kcal/mol	$\Delta S^\ddagger$, eu
H			20.2 (3)	−17.1 (7)
	32	3.55 (10)		
	48	19.6 (6)		
	59	60.4 (13)		
CH_3			21.6 (3)	−14.1 (6)
	32	1.69 (12)		
	48	11.2 (4)		
	59	34.9 (9)		
CF_3			20.3 (6)	−17.9 (17)
	32	2.07 (8)		
	48	12.2 (6)		
	59	35.8 (13)		
$N(CH_3)_2$			22.0 (4)	−12.4 (11)
	32	2.16 (9)		
	48	15.5 (6)		
	59	46.3 (13)		

Table V. Crystal Data for $Cp^*(\eta^5,\eta^1\text{-}C_5Me_4CH_2)HfCH_2C_6H_5$ (9)

formula $HfC_{27}H_{36}$	fw 539.08
space group $P\bar{1}$	T = 21 °C
Z = 2	V = 1161 (1) Å^3
a = 9.084 (2) Å	
b = 10.492 (2) Å	ρ_{calcd} = 1.543 (1) g/cm^3
c = 12.328 (1) Å	
	$\bar{\nu}$(Mo Kα) = 47.5 cm^{-1}
α = 95.81 (1)°	μr_{max} = 1.70
β = 96.60 (1)°	
γ = 91.15 (2)°	λ(Mo Ka) = 0.710 73 Å
	$F(000)$ = 540 e
	cryst size 0.55 × 0.31 × 0.34 mm

Table VI. Final Parameters[a]

	x	y	z	U_{eq}[b]
Hf	2076.9 (3)	1815.0 (3)	2536.0 (2)	30.6 (1)
C11	3978 (8)	1619 (8)	4177 (6)	43 (2)
C12	3182 (8)	421 (8)	3949 (6)	46 (2)
C13	3510 (8)	−152 (7)	2918 (6)	43 (2)
C14	4532 (8)	667 (7)	2521 (6)	41 (2)
C15	4775 (7)	1776 (7)	3279 (6)	39 (2)
C11M	4250 (10)	2401 (10)	5265 (7)	67 (3)
C12M	2344 (11)	−213 (10)	4729 (9)	73 (3)
C13M	2971 (11)	−1439 (9)	2369 (8)	67 (3)
C14M	5393 (10)	315 (10)	1577 (7)	61 (2)
C15M	5889 (9)	2855 (9)	3222 (8)	62 (2)
C21	771 (9)	3245 (8)	3721 (7)	48 (2)
C22	1629 (9)	4155 (7)	3240 (6)	45 (2)
C23	1106 (8)	4050 (7)	2114 (7)	45 (2)
C24	−15 (8)	3080 (8)	1879 (7)	44 (2)
C25	−166 (8)	2520 (8)	2899 (7)	47 (2)
C21M	761 (11)	3157 (11)	4942 (7)	68 (3)
C22M	2660 (11)	5199 (9)	3805 (8)	66 (3)
C23M	1531 (11)	4949 (8)	1320 (8)	61 (2)
C24M	−1005 (9)	2755 (9)	831 (8)	61 (2)
C25M	−256 (9)	1133 (9)	2876 (8)	58 (2)
C31	2395 (9)	2036 (8)	−149 (6)	48 (2)
C32	1491 (12)	2100 (10)	−1124 (7)	67 (3)
C33	1852 (20)	2879 (15)	−1896 (9)	107 (5)
C34	3154 (24)	3572 (14)	−1746 (13)	119 (5)
C35	4073 (17)	3515 (12)	−797 (13)	101 (4)
C36	3703 (12)	2770 (9)	9 (8)	67 (2)
C31M	1999 (9)	1197 (8)	685 (6)	48 (2)

[a] x, y, and $z \times 10^4$; $U_{eq} \times 10^3$ Å^2. [b] $U_{eq} = {}^1/_3\sum_i\sum_j U_{ij}(a_i^*a_j^*)\mathbf{a}_i^*\cdot\mathbf{a}_j^*$; $\sigma(U_{eq}) = 6^{-1/2}\langle \sigma U_{ii}/U_{ii}\rangle U_{eq}$.

of yellow-orange **12**. Anal. Calcd for $HfC_{29}H_{41}N$: C, 59.83; H, 7.10; N. 2.41. Found: C, 60.23; H, 7.17; N, 2,19.

Kinetic Measurements of Thermal Decomposition. With the exception of **2b**, all reactions were followed by monitoring the decrease in height of the pentamethylcyclopentadienyl resonance of starting complex relative to internal $(\eta^5\text{-}C_5H_5)_2Fe$. The rate of decomposition of **2b** was followed by monitoring the decrease in integrated intensity of the $(Cp^*\text{-}d_{15})_2Hf(C\mathit{H}_2C_6H_5)_2$ signal relative to $(\eta^5\text{-}C_5H_5)_2Fe$. NMR spectra were recorded at timed intervals by using a Varian EM-390 (90-MHz) spectrometer. Reaction temperatures were maintained by using constant temperature oil baths controlled by thermoregulators and were observed to be constant to within ±1 °C. A typical experiment involved 25 mg of hafnium complex and 6–10 mg of ferrocene dissolved in 0.4 mL of benzene-d_6. The NMR tubes were sealed containing >1 atm of dinitrogen. Total submersion in the oil bath

Table VII. Selected Distances (Å) and Angles (deg)[a]

Bond Distances			
Hf–C21	2.412 (8)	C22–C23	1.407 (11)
Hf–C22	2.576 (8)	C22–C22M	1.489 (13)
Hf–C23	2.603 (8)	C23–C24	1.410 (11)
Hf–C24	2.448 (8)	C23–C23M	1.501 (12)
Hf–C25	2.258 (8)	C24–C25	1.460 (11)
Hf–C25M	2.320 (9)	C24–C24M	1.492 (12)
Hf–C31M	2.301 (8)	C25–C25M	1.453 (12)
C21–C22	1.436 (11)	Hf–Cp*1	2.224
C21–C25	1.396 (11)	Hf–Cp*2	2.146
C21–C21M	1.519 (13)		

Bond Angles			
C22–C21–C25	109.7 (7)	C21C25–C24	106.5 (7)
C22–C21C21M	125.7 (7)	C21–C25–C25M	120.1 (7)
C25–C21–C21M	124.4 (7)	C24–C25–C25M	118.8 (7)
C21–C22–C23	106.6 (7)	C31M–Hf–C25M	101.5 (3)
C21–C22–C22M	128.4 (7)	Cp*1–Hf–Cp*2	141.6
C23–C22–C22M	124.0 (7)	Cp*1–Hf–C25M	116.3
C22–C23–C24	109.5 (7)	Cp*1–Hf–C31M	107.0
C22–C23–C23M	125.0 (7)	Cp*2–Hf–C25M	69.1
C24–C23–C23M	125.1 (7)	Cp*2–Hf–C31M	108.9
C23–C24–C25	107.3 (7)	Cp*2–C25–C25M	142.7
C23–C24–C24M	127.7 (7)	C25–Cp*2–Hf	79.0
C25–C24–C25M	124.6 (7)	C25M–Cp*2–Hf	58.7

[a] Cp*1 and Cp*2 are the centroid coordinates of C11 through C15 and C21 through C25 Cp* rings, respectively.

prevented the benzene-d_6 from refluxing at the elevated temperatures used in this study. Peak heights were demonstrated to be reproducible to within ±7% by repeated measurement. Each spectrum was recorded three times, and the average peak height was used to calculate the values of k given in Tables I, II, and IV. Errors in k represent approximately one standard deviation. Plots of $\ln (k/T)$ vs. $1/T$ were constructed from the decomposition rates and yielded the activation parameters $\Delta H^{\ddagger}$ and $\Delta S^{\ddagger}$. Errors in $\Delta H^{\ddagger}$ and $\Delta S^{\ddagger}$ represent one standard deviation calculated by error propagation of one standard deviation changes in the value of $-\Delta H^{\ddagger}/R$ and $\ln (A/T) - 1$, when the measured k values are varied within their error limits.

X-ray Structure Determination. Crystals of $(\eta^5\text{-}C_5Me_5)(\eta^5,\eta^1\text{-}C_5Me_4CH_2)HfCH_2C_6H_5$ (**9**) were obtained by slow evaporation of a saturated diethyl ether solution and sealed in glass capillaries under dinitrogen to prevent decomposition. Oscillation and zero-, first-, and second-layer Weissenberg photographs showed no evidence of twinning, and the crystal was mounted on a CAD4 diffractometer equipped with graphite-monochromated Mo Kα radiation. A least-squares fit to the setting angles of 25 reflections (20 of which were independent of one another) with $16° < 2\theta < 26°$ indicated a triclinic cell and yielded the cell parameters. As neither nontrivial symmetry nor systematic absences were observed in the photographs, and since an approximate calculation indicated two molecules per cell, $P\bar{1}$ symmetry was assumed. All data ($\pm h,\pm k,\pm l$) with $2° < 2\theta < 52°$ were collected, and the $hk0$ reflections were collected twice. These data were merged to give 4529 independent observations. Three index reflections monitored every 10000 s of X-ray exposure time showed a linear decay of 1.5% in F over the 136 h required to collect the data. The data were corrected for this decay, as well as for Lorentz and polarization factors, but no correction was made for absorption due to the rounded shape of the crystal, which made an accurate representation of its shape impractical.

Solution and Refinement. A Wilson plot was used to place the data on an approximately absolute scale. Variances, $\sigma^2(I)$, were assigned to the intensities on the basis of counting statistics plus an additional term, $(0.014I)^2$, to account for additional errors proportional to the intensity. A Patterson map yielded hafnium coordinates and successive structure factor–Fourier calculations located the remaining atoms. Refinement with all the heavy atoms anisotropic converged with $R = \sum||F_o| - |F_c||/\sum|F_o| = 0.048$ for all 4455 reflections with $F_o^2 > 0$ and 0.046 for the 4187 reflections with $F_o^2 > 3\sigma(F_o^2)$. The goodness-of-fit, $[\sum w(F_o^2 - F_c^2)/(n - p)]^{1/2}$, where n = number of data = 4529 and p = number of parameters = 254, is 4.37.[27] Idealized hydrogen atoms were introduced during the refinement and repositioned two or three times, depending on the accuracy of the initial placement. Non-methyl hydrogen positions were calculated in accordance with expected bond geometry; methyl hydrogens were placed on the basis of Fourier maps in the plane where they were expected. At first the maps did not clearly suggest all hydrogen positions, but by the last cycle the idealized positions where the hydrogens were placed agreed fairly closely with the difference maps. All hydrogens were assigned isotropic temperature factors 1.0 Å^2 greater than the equivalent isotropic factors of the parent carbons. In the final least squares cycle no parameter shifted by more than 0.03 of its standard deviation. Crystal data are given in Table V and final parameters in Table VI. Calculations were done by using the programs of the CRYM crystallographic computing system[28] on a VAX 11/750 computer; the drawing was done by using ORTEP.[29]

Acknowledgment. We wish to thank Allan van Asselt for valuable contributions to this research. This work was supported by the National Science Foundation (Grant CHE-8303735), by the USDOE Office of Energy Research, Office of Basic Energy Sciences (Grant No. DE-FG03-85ER13431), and by Shell Companies Foundation, which are gratefully acknowledged.

Registry No. **1**, 85959-83-7; **2**, 107681-81-2; **3**, 107681-82-3; **4**, 107681-83-4; **5**, 107681-84-5; **6**, 107681-85-6; **7**, 107681-86-7; **9**, 107681-88-9; **11**, 107681-89-0; **12**, 107681-90-3; **13**, 107711-12-6; **14**, 107711-13-7; **15**, 107711-14-8; **16**, 107681-91-4; $(Cp^*\text{-}d_{15})_2HfI_2$, 107681-87-8; $C^*_2HfH_2$, 81956-87-8; $Cp^*_2HfI_2$, 92786-75-9; $KCH_2C_6H_5$, 2785-29-7; $KCH_2C_6H_4\text{-}m\text{-}CH_3$, 55301-51-4; $KCH_iC_6H_4\text{-}m\text{-}NMe_2$, 107681-92-5; $LiCH_2CMe_3$, 7412-67-1; $ClMgCH_2C_6H_4\text{-}m\text{-}CF_3$, 107549-19-9; D_2, 7782-39-0.

Supplementary Material Available: Tables of complete bond lengths and angles, methyl hydrogen idealized positional parameters, and thermal parameters and a stereoview of $(\eta^5\text{-}C_5Me_5)(\eta^5,\eta^1\text{-}C_5Me_4CH_2)HfCH_2C_6H_5$ (5 pages); a listing of structure factors (20 pages). Ordering information is given on any current masthead page.

---

(27) The absorption correction was only approximate because of the irregular shape of the crystal. Because of this, there are large excursions near the hafnium atom in the final difference map (+5.05, −3.43 e Å^3). The high value of the goodness-of-fit probably results from this also. We believe the weights were chosen properly; a larger "fudge" factor for them (such as 0.05 rather than the 0.02 we used) would improve the goodness of fit, but such a high value is not indicated by the data.

(28) Duchamp, D. J. CRYM Crystallographic Computing System; American Crystallographers Association Meeting, Bozeman, MT, 1964; Paper B14, p 29.

(29) Johnson, C. K. ORTEP, Report ORNC-3794; Oak Ridge National Laboratory, Oak Ridge, TN, 1965.